Determining the spring constant of arbitrarily shaped cantilevers in viscous environments

A. F. Payam, W. Trewby, and K. Voïtchovsky

Citation: Appl. Phys. Lett. **112**, 083101 (2018); doi: 10.1063/1.5009071
View online: https://doi.org/10.1063/1.5009071
View Table of Contents: http://aip.scitation.org/toc/apl/112/8
Published by the American Institute of Physics

Determining the spring constant of arbitrarily shaped cantilevers in viscous environments

A. F. Payam,[a] W. Trewby,[a] and K. Voïtchovsky[b]
Department of Physics, Durham University, Durham DH1 3LE, United Kingdom

(Received 12 October 2017; accepted 7 February 2018; published online 20 February 2018)

Accurate calibration of the flexural spring constant of microcantilevers is crucial for sensing devices, microactuators, and atomic force microscopy (AFM). Existing methods rely on precise knowledge of cantilever geometry, make significant simplifications, or require potentially damaging contact with the sample. Here, we develop a simple equation to calculate the flexural spring constants of arbitrarily shaped cantilevers in fluid. Our approach, verified here with AFM, only requires the measurement of two resonance frequencies of the cantilever in air and in a liquid, with no need for additional input or knowledge about the system. We validate the method with cantilevers of different shapes and compare its predictions with existing models. We also show how the method's accuracy can be considerably improved, especially in more viscous liquids, if the effective width of the cantilever is known. Significantly, the developed equations can be extended to calculate the spring constants of the cantilever's higher eigenmodes. https://doi.org/10.1063/1.5009071

Microcantilevers constitute the backbone of a wide range of technologies, from actuators in MEMS[1] to sensors[2] and lab-on chip technology,[3] and for atomic force microscopy (AFM).[4] Microcantilever-based measurements of forces with pico-Newton resolution and of displacements down to the Ångström level are now commonplace. Most applications rely on small relative displacements or bending of the lever, which can generally be modelled by a linear spring with a single flexural spring constant, k_f. Precise knowledge of k_f is hence key to achieving accurate and reproducible results, and considerable efforts have been dedicated to the modelling of cantilevers' motion[5] and to the development of calibration procedures.[6] The task is, however, highly challenging because accurate predictions require precise knowledge of the cantilever's geometrical and physical characteristics, something far from trivial, given manufacturing variability at that scale. Additionally, no single model works for all cantilever geometries, let alone unusual and arbitrary shapes, unless considerable simplifications are made.[7] To add to this complexity, the dynamical properties of cantilevers on which most models rely strongly depend on the viscoelastic properties of the immediate environment.

In the field of AFM, the need for accurate k_f characterization is a central issue, given the use of microcantilevers to measure minute molecular[8–10] or interfacial forces,[11–13] often close to the thermal limit. It also feeds into the problem of force-reconstruction, where the spatial landscape of a force potential is calculated from dynamical measurements with a vibrating cantilever.[14–19] Perhaps unsurprisingly, many AFM-based methods have been proposed to estimate k_f based on the dynamic motion of the cantilever, typically measured by a laser focused near the cantilever's free extremity.[6,20–30] To date, the most common methods are the so-called thermal noise method[21,31,32] and the Sader method[18,22,23,30,33]—a comprehensive review of most of the methods available can be found in Ref. 6.

The thermal noise method is derived from equipartition theory and requires knowledge of the frequency-dependent response of the cantilever to thermal fluctuations in the surrounding environment [i.e., the thermal spectrum, see Fig. 1(a)].[21,32] If the inverse optical lever sensitivity (invOLS) of the cantilever-laser system is known, fitting of the thermal spectrum can be used to find k_f for any resonant mode of the cantilever. The method's accuracy depends on mechanical noises and white noise from the environment. The result is also highly sensitive to the choice of interval used to fit the relevant portion of the thermal spectrum. Significantly, the measurement of the invOLS usually requires bending the cantilever on a hard substrate, a procedure that can damage or permanently alter the measuring tip. This can, in principle, be avoided by calibrating the invOLS after an experiment, at the cost of uncertainties in the forces applied to the sample of interest.

The Sader method, developed by John E. Sader,[18,22,23,30,33] is also based on the thermal spectrum of the cantilever but relies on a more sophisticated fitting procedure that takes into account the fundamental resonance frequency of the cantilever, its quality (Q) factor, geometrical shape, and hydrodynamic function. The method works for cantilevers with rectangular or V-shaped geometries[22] [see Fig. 1(b)]. It can be adapted to other shapes but requires the input of cantilever-dependent parameters that are not readily measurable.[22]

Both the thermal noise and Sader methods have become benchmarks in the field; they can be implemented in air or liquid environments but often lead to different results due to strongly enhanced—and often tip-sample-separation dependent—damping in fluid environments. Prediction errors can become significant in highly viscous environments, partly

[a]A. F. Payam and W. Trewby contributed equally to this work.
[b]Author to whom correspondence should be addressed: kislon.voitchovsky@durham.ac.uk

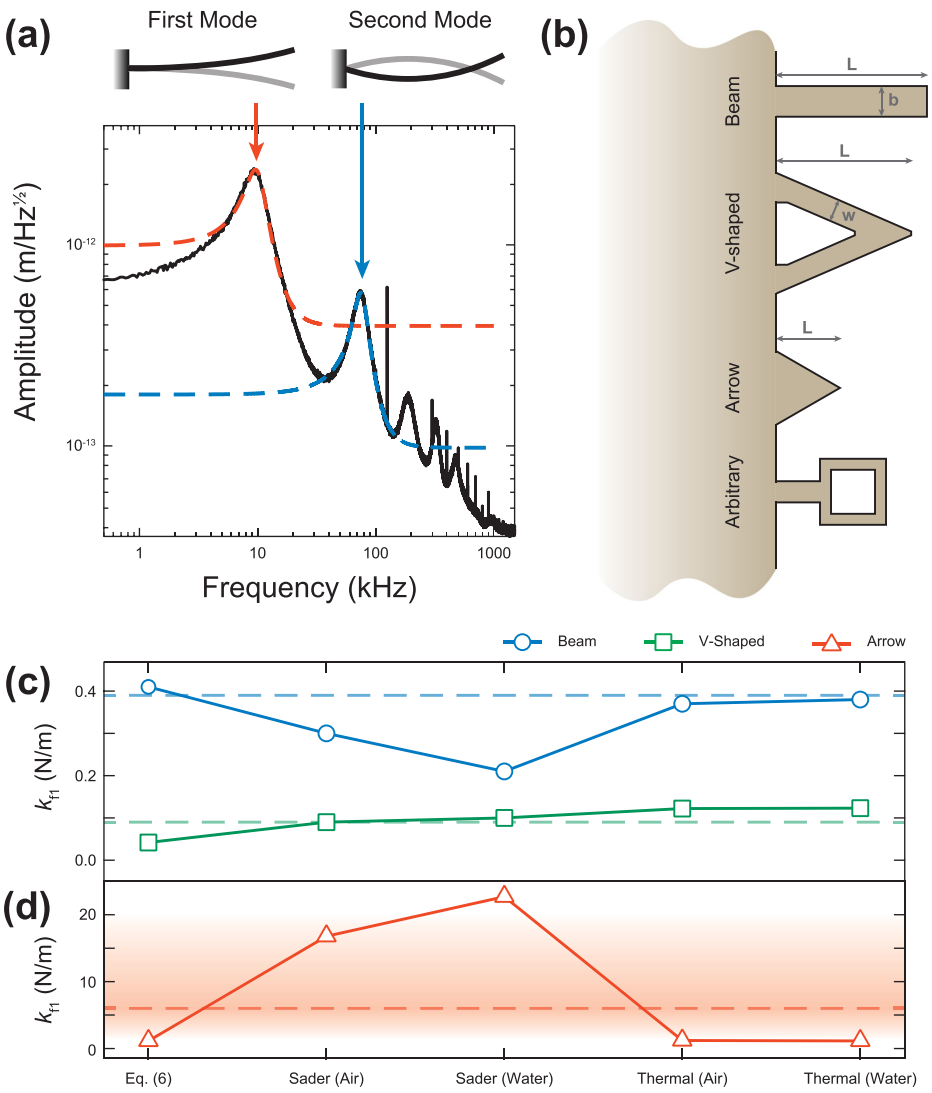

FIG. 1. Calculation of the flexural spring constants from cantilever dynamics. (a) Thermal spectrum recorded with a V-shaped cantilever immersed in water. The first two resonance peaks are highlighted and the corresponding modes of oscillation. Simple harmonic oscillator model fits are shown for the first and second modes as red and blue dashes, respectively. (b) Examples of differently shaped cantilevers and the relevant dimensions used in theoretical models. The upper three types are investigated in this study. The lower cantilever exemplifies a shape that would represent a challenge for traditional methods. (c) Flexural spring constant, k_f, predicted by Eq. (6), the Sader method, and the thermal method for a beam and V-shaped cantilever in air and water. Nominal manufacturer's values are highlighted with dashed lines. In general, Eq. (6) produces results consistent with the manufacturer's values and those measured via the thermal method. In the case of the beam, Eq. (6) appears to give more robust results than the Sader model in both air and water. (d) Flexural spring constants predicted by the various models for an arrow-shaped cantilever. Here, there is no good agreement between the (poorly defined) nominal stiffness and any model, but Eq. (6) again agrees well with the thermal method. The red gradient here reflects the manufacturer's broad nominal stiffness range ($k_f \sim 6$ N/m typical, with 1.5 N/m $< k_f <$ 20.0 N/m). Calculated errors for Eq. (6) are smaller than the data markers.

due to difficulties in accurately measuring a quality factor. Moreover, for cantilevers with non-standard geometry [Fig. 1(b)], the Sader method requires further adjustments.[22]

Here, we propose a method for calibrating the flexural stiffness of cantilevers with arbitrary shapes in viscous fluids. Our approach requires only knowledge of the cantilever's length and its first two resonant frequencies in air and liquid. There is no dependence on the cantilever's quality factor, no need for invOLS calibration, and results in air or viscous liquids are comparable or more accurate than with the existing methods. If the effective width of the cantilever is known, we show that the accuracy of the predictions can be further improved over established methods with the knowledge of only first resonance frequencies of the cantilever in air or desired liquid.

Our method begins from the dynamic motion of the cantilever based on the Euler-Bernoulli partial differential equation[34]

$$EI\frac{\partial^4}{\partial x^4}W(x,\,t)+\rho_c bh\frac{\partial^2}{\partial t^2}W(x,\,t)=F_{\rm exc}+F_h, \qquad (1)$$

where E is the cantilever's Young's modulus, I is its rotary inertia, ρ_c is the cantilever density, and b and h are the width and thickness of the cantilever, respectively. $W(x,\,t)$ is the time-dependent displacement of the cantilever, $F_{\rm exc}$ is the excitation force, and F_h is the hydrodynamic force which can be described by a separate added mass and damping stiffness. Considering the added mass and damping stiffness per unit length of the cantilever[34–36] and assuming a hydrodynamic function characterized by two real (a_1 and a_2) and two imaginary (b_1 and b_2) regression coefficients,[35,37,38] we can relate the angular resonance frequencies of the microcantilever in air, ω_{an}, and in an arbitrary fluid, $\omega_{{\rm f}n}$,[39] for any given mode n:

$$\omega_{{\rm f}n}^2\left(\frac{\pi a_1\rho_{\rm f}b}{4\rho_c h}+1\right)+\omega_{{\rm f}n}^{3/2}\left(\frac{\pi a_2\sqrt{\eta\rho_{\rm f}}}{2\rho_c h}\right)=\omega_{an}^2, \qquad (2)$$

where $\rho_{\rm f}$ and η are the density and the viscosity of the fluid, respectively.

The hydrodynamic coefficients a_i and b_i are independent of the cantilever characteristics or the medium in which it operates, have been evaluated elsewhere, and can be assumed to be constant for different cantilevers.[35,37,38] After measuring two resonance frequencies of the cantilever in both air and a liquid environment from the thermal spectrum [Fig. 1(a)], the areal mass density, $\rho_c h$, and width, b, can be obtained from Eq. (2)

$$\widehat{\rho_c h}=\frac{\pi a_2\sqrt{\rho_{\rm f}\eta}}{2}\frac{\omega_{\rm f1}^{3/2}\omega_{\rm f2}^{3/2}\left(\sqrt{\omega_{\rm f2}}-\sqrt{\omega_{\rm f1}}\right)}{\left(\omega_{a1}^2-\omega_{\rm f1}^2\right)\omega_{\rm f2}^2-\left(\omega_{a2}^2-\omega_{\rm f2}^2\right)\omega_{\rm f1}^2}, \qquad (3)$$

$$\widehat{b} = \frac{2a_2\sqrt{\eta}}{a_1\sqrt{\rho_f\omega_{f1}}}\left(\frac{\omega_{f2}^{3/2}\left(\sqrt{\omega_{f2}}-\sqrt{\omega_{f1}}\right)\left(\omega_{a1}^2-\omega_{f1}^2\right)}{\left(\omega_{a1}^2-\omega_{f1}^2\right)\omega_{f2}^2-\left(\omega_{a2}^2-\omega_{f2}^2\right)\omega_{f1}^2}-1\right). \tag{4}$$

Here, the carat denotes a calculated value and the indices a and f refer to the eigenfrequencies of the cantilever in air and in a fluid, respectively. The flexural spring constant, k_{fn}, of each mode of the cantilever is related to the effective mass of that mode, m_n, through the relation $k_{fn} = m_n\omega_{an}^2$,[40] and the effective mass can be found from the actual mass, m_c, or the cantilever's geometrical parameters by[40]

$$m_n = \frac{1}{4}m_c = \frac{1}{4}\rho_c hbL, \tag{5}$$

where L represents the cantilever length. By combining Eqs. (3)–(5), we obtain the following expression for the cantilever's first mode spring constant

$$k_{f1} = \frac{1}{4}\widehat{\rho_c h}\widehat{b}L\omega_{a1}^2. \tag{6}$$

Figure 1(c) compares k_{f1} predictions obtained from Eq. (6), the thermal and Sader methods for the beam (RC800 PSA, Olympus), and V-shaped (TR400 PB, Olympus) cantilevers, in air and in water. For the beam cantilever, Sader's equation (1) in Ref. 22 is used, and for the V-shaped cantilever, we use the adapted equation (8) in the same paper. In each case, the cantilever's nominal values are shown as dashed lines for reference. The predictions obtained from Eq. (6) broadly agree with the thermal method and are as accurate as the Sader method in most cases if the nominal value is taken as a reference point. We note that there is no independent measurement of cantilever stiffness here—even manufacturer's values are typically given with large uncertainties —and so, there is no formal measure of accuracy for our model. The proximity of the thermal method and nominal values does imply that our results are accurate. However, unlike the thermal method, Eq. (6) does *not* require invOLS calibration with the potentially damaging tip-sample contact. The Sader method is closer to both the nominal value and the thermal method than Eq. (6) for the V-shaped cantilever. However, we note that the equation used here required two hydrodynamic coefficients (a_1 and a_2) specially developed for V-shaped cantilevers and, as such, is not applicable to arbitrary cantilevers. Further validation of our model for cantilevers of different geometries and stiffness is shown in Table SI of the supplementary material.

For arrow-shaped cantilevers (Arrow UHF AuD, Nanoworld), the parallel beam approximation developed by Sader cannot be easily adapted, and so, we make use of Eq. (1) in Ref. 22. We again find an excellent agreement between Eq. (6) and the thermal method [less than 7%, see Fig. 1(d)], demonstrating the validity of the approach. The broad range of nominal values, indicated by the red gradient in Fig. 1(d), is a result of the complex geometry of the arrow cantilever used (see Fig. S1 in the supplementary material). This suggests significant variability in the manufacturing and further emphasises the need for accurate calibration methods that are not based on nominal values.

There is however one caveat to Eq. (6): the viscosity of the environment in which the cantilever operates. Most models that use dynamical measurements to find a value for k_f tend to fail when the measurements are conducted in highly viscous environments, and Eq. (6) is no exception. The results presented in Fig. 1 are based on measurements conducted in a relatively low viscosity environment—air and pure water. However, when working in more viscous liquids and especially with softer cantilevers, the quality of the predictions progressively decreases (Fig. 2). This is a problem for applications such as viscometry or biosensing[39] where microcantilevers are used in non-Newtonian bodily fluids. To overcome this issue, we developed a more accurate equation for predicting k_f. This comes at the cost of an extra parameter needed as an input: the width b of the cantilever or an effective width for non-rectangular cantilevers. If b is known, the areal mass density of the cantilever $\widehat{\rho_c h}$ becomes

$$\widehat{\rho_c h} = \frac{\omega_{f1}^2\pi a_1\rho_f b + 2\omega_{f1}^{3/2}\pi a_2\sqrt{\rho_f\eta}}{4\left(\omega_{a1}^2-\omega_{f1}^2\right)}, \tag{7}$$

which, using Eq. (5), yields the following expression for k_{f1}:

$$k_{f1} = \frac{\omega_{f1}^2\pi a_1\rho_f b + 2\omega_{f1}^{3/2}\pi a_2\sqrt{\rho_f\eta}}{16\left(\omega_{a1}^2-\omega_{f1}^2\right)}bL\omega_{a1}^2. \tag{8}$$

Significantly, Eq. (8) does not depend on the Q factor of the cantilever, making it less sensitive to the difficulties in measuring Q accurately in viscous environments. We also note that Eq. (8) only requires the frequency of the first resonance of the cantilever, another advantage in viscous media. We tested Eq. (8) in five fluids of varying viscosity: ultrapure water, isopropanol, acetone, butanol, decane, and hexanol (Sigma-Aldrich, Dorset, UK, purity >99%). The measurements were conducted with a rectangular cantilever (Olympus RC800 PSA)

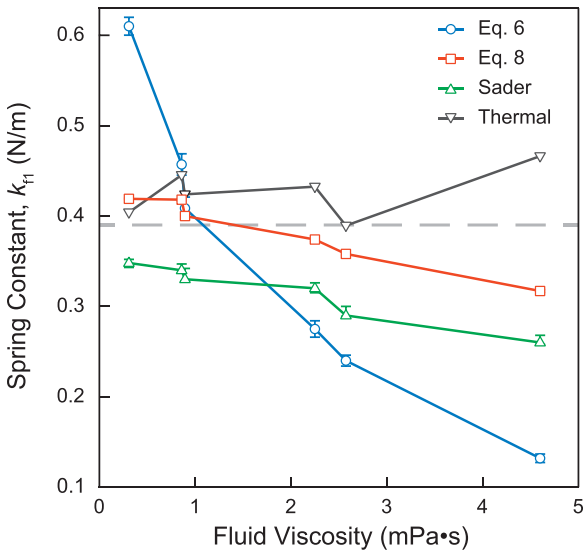

FIG. 2. Assessment of the impact of the surrounding fluid's viscosity on the predicted spring constant of a beam cantilever. The thermal method is reasonably constant with viscosity as expected but deviates from the nominal manufacturer's value (dashed line) of 0.39 N/m. In contrast, both Eq. (6) and the Sader method vary, decreasing as the viscosity increases. Equation (8) performs much better, returning a more stable value for k_f that is consistent with the thermal method and has reduced errors at all but the highest viscosities.

and compared with predictions from Eq. (6), Sader, and the thermal method; the results can be seen in Fig. 2.

The results show that the stiffness as calculated via Eq. (8) is less sensitive to viscosity than the other methods, whereas Eq. (6) fails dramatically, with around 70% variation. The Sader method's results decrease with viscosity and are offset from both the thermal method and nominal values. This reflects the dependence of the method on the Q-factor, which tends to vary dramatically with the fluid viscosity. Together, these results validate Eq. (8) and show that it provides the most reliable model for calculating k_f, particularly when operating in highly viscous environments.

In this paper, we propose an approach to determine the spring constant of a cantilever based solely on the measurement of its two first eigenfrequencies. The method does not require any knowledge about cantilever characteristics, making it particularly useful for calibration of systems where accurate determination of the geometry or shape is not possible. Significantly, comparison with existing popular methods shows that our approach provides similar or better results. We show that if the width of the cantilever is known, the quality of the prediction can be further improved, especially in viscous fluids where other methods tend to fail. Our equations can also be extended to determine spring constants of higher eigenmodes of vibrating cantilevers, a key to multimodal measurements including in the fast growing field of multifrequency AFM.[41,42]

See supplementary material for a list of the measured parameters used in Fig. 1, additional measurements with different cantilevers in viscous liquids, and a detailed description of the experimental methodology, including error calculations.

This work was supported by the Engineering and Physical Sciences Research Council (Grant No. 1452230), the Biotechnology and Biological Science Research Council (Grant No. BB/M024830/1), and the European Council (FP7 CIG 631186). Insightful discussions with Clodomiro Cafolla are gratefully acknowledged.

[1]S. Beeby, *MEMS Mechanical Sensors* (Artech House, Boston, 2004).
[2]R. Datar, S. Kim, S. Jeon, P. Hesketh, S. Manalis, A. Boisen, and T. Thundat, MRS Bull. **34**, 449 (2009).
[3]N. McLoughlin, S. L. Lee, and G. Hahner, Appl. Phys. Lett. **89**, 184106 (2006).
[4]F. J. Giessibl, Rev. Mod. Phys. **75**, 949 (2003).
[5]A. Raman, J. Melcher, and R. Tung, Nanotoday **3**, 20 (2008).
[6]C. T. Gibson, D. A. Smith, and C. J. Roberts, Nanotechnology **16**, 234 (2005).
[7]J. P. Cleveland, S. Manne, D. Bocek, and P. K. Hansma, Rev. Sci. Instrum. **64**, 403 (1993).
[8]K. Voitchovsky, J. J. Kuna, S. A. Contera, E. Tosatti, and F. Stellacci, Nat. Nanotechnol. **5**, 401 (2010).
[9]D. Ortiz-Young, H.-C. Chiu, S. Kim, K. Voïtchovsky, and E. Riedo, Nat. Commun. **4**, 2482 (2013).
[10]K. Voitchovsky, Nanoscale **8**, 17472 (2016).
[11]R. Garcia and R. Perez, Surf. Sci. Rep. **47**, 197 (2002).
[12]A. Elbourne, K. Voïtchovsky, G. G. Warr, and R. Atkin, Chem. Sci. **6**, 527 (2015).
[13]J. J. Kuna, K. Voïtchovsky, C. Singh, H. Jiang, S. Mwenifumbo, P. K. Ghorai, M. M. Stevens, S. C. Glotzer, and F. Stellacci, Nat. Mater. **8**, 837 (2009).
[14]H. Hölscher, Appl. Phys. Lett. **89**, 123109 (2006).
[15]A. F. Payam, D. Martin-Jimenez, and R. Garcia, Nanotechnology **26**, 185706 (2015).
[16]S. Hu and A. Raman, Nanotechnology **19**, 375704 (2008).
[17]A. J. Katan, M. H. van Es, and T. H. Oosterkamp, Nanotechnology **20**, 165703 (2009).
[18]J. E. Sader and S. P. Jarvis, Appl. Phys. Lett. **84**, 1801 (2004).
[19]J. E. Sader, T. Uchihashi, M. J. Higgins, A. Farrell, Y. Nakayama, and S. P. Jarvis, Nanotechnology **16**, S94 (2005).
[20]C. T. Gibson, G. S. Watson, and S. Myhra, Nanotechnology **7**, 259 (1996).
[21]R. Lévy and M. Maaloum, Nanotechnology **13**, 33 (2002).
[22]J. E. Sader, J. A. Sanelli, B. D. Adamson, J. P. Monty, X. Wei, S. A. Crawford, J. R. Friend, I. Marusic, P. Mulvaney, and E. J. Bieske, Rev. Sci. Instrum. **83**, 103705 (2012).
[23]J. E. Sader and L. White, J. Appl. Phys. **74**, 1 (1993).
[24]N. R. Shatil, M. E. Homer, L. Picco, P. G. Martin, and O. D. Payton, Appl. Phys. Lett. **110**, 223101 (2017).
[25]J. E. Sader, J. W. M. Chon, and P. Mulvaney, Rev. Sci. Instrum. **70**, 3967 (1999).
[26]J. Lübbe, L. Doering, and M. Reichling, Meas. Sci. Technol. **23**, 45401 (2012).
[27]C. A. Clifford and M. P. Seah, Nanotechnology **16**, 1666 (2005).
[28]J. R. Lozano, D. Kiracofe, J. Melcher, R. Garcia, and A. Raman, Nanotechnology **21**, 465502 (2010).
[29]J. W. M. Chon and P. Mulvaney, J. Appl. Phys. **87**, 3978 (2000).
[30]C. P. Green, H. Lioe, J. P. Cleveland, R. Proksch, P. Mulvaney, and J. E. Sader, Rev. Sci. Instrum. **75**, 1988 (2004).
[31]J. L. Hutter and J. Bechhoefer, Rev. Sci. Instrum. **64**, 1868 (1993).
[32]H.-J. Butt and M. Jaschke, Nanotechnology **6**, 1 (1995).
[33]J. E. Sader, J. Pacifico, C. P. Green, and P. Mulvaney, J. Appl. Phys. **97**, 124903 (2005).
[34]A. F. Payam, Ultramicroscopy **135**, 84 (2013).
[35]S. Basak, A. Raman, and S. V. Garimella, J. Appl. Phys. **99**, 114906 (2006).
[36]R. C. Tung, J. P. Killgore, and D. C. Hurley, Rev. Sci. Instrum. **84**, 073703 (2013).
[37]A. F. Payam and M. Fathipour, Micron **70**, 50 (2015).
[38]A. Maali, C. Hurth, R. Boisgard, C. Jai, T. Cohen-Bouhacina, and J. Aimé, J. Appl. Phys. **97**, 074907 (2005).
[39]A. F. Payam, W. Trewby, and K. Voïtchovsky, Analyst **142**, 1492 (2017).
[40]J. R. Lozano and R. Garcia, Phys. Rev. B **79**, 014110 (2009).
[41]R. Garcia and E. T. Herruzo, Nat. Nanotechnol. **7**, 217 (2012).
[42]C. A. Amo, A. P. Perrino, A. F. Payam, and R. Garcia, ACS Nano **11**, 8650 (2017).